40

44

The State Scientific Center of Russia

The Budker Institute of Nuclear Physics
SB RAS

J.G. Körner, K. Melnikov, O.I. Yakovlev

TWO-LOOP $O(G_F M_H{}^2)$ RADIATIVE CORRECTIONS TO THE HIGGS DECAY WIDTH $H \to \gamma\gamma$ FOR LARGE HIGGS BOSON MASSES

Budker INP 95-68

НОВОСИБИРСК

Two–loop $O(G_F M_H{}^2)$ radiative corrections to the Higgs decay width $H \to \gamma\gamma$ for large Higgs boson masses

J. G. Körner[1,2,3], *K. Melnikov*[1,4], *and O. I. Yakovlev*[1,5]

Abstract

This note is devoted to the calculation of the two-loop $O(G_F M_H{}^2)$ radiative corrections to the Higgs decay width $H \to \gamma\gamma$ for large values of the Higgs boson mass M_H within the Minimal Standard Model. The use of the Equivalence Theorem makes it possible to reduce the problem to the consideration of the physical Higgs boson field and the Goldstone bosons w^+, w^-, z. We present analytical results for the various two- and three-particle absorptive parts of two-loop contributions, using dispersive techniques, analytic results for all but one of the dispersive contributions. The typical size of the correction is $\sim$ 30 percent for a Higgs boson mass of order 1 TeV.

[1] Institut für Physik, THEP, Johannes Gutenberg Universität, Staudinger Weg 7, Mainz D 55099, Germany.

[2] Supported by the BMFT, FRG, under contract 06MZ566

[3] Supported in part by Human Capital and Mobility program, EU, under contract CHRX-CT94-0579

[4] Supported by Graduiertenkolleg "Teilchenphysik", Mainz

[5] The State Scientific Center Budker Institute of Nuclear Physics, 630090, Novosibirsk, Russia

1.Introduction

The neutral scalar Higgs boson is the essential ingredient of the Standard Model of the electroweak interactions. The Higgs boson mass is a free parameter in the Minimal Standard Model and until now we do not know much about its value. Experiments exclude a Higgs boson lighter then $\sim$ 65 GeV. Also theoretical arguments based on perturbative unitarity suggest that the upper bound on the Higgs boson mass is $O(1)$ TeV [6].

It is widely believed that the properties of the Higgs boson can be investigated at the Next Linear Collider which will be able to operate in different modes ($e^+e^-, e^{+;-}\gamma, \gamma\gamma$). In particular $\gamma\gamma$ collisions are well suited not only for the observation of the Higgs boson signal but also for studying its properties (for a review see Ref. [2]).

As is known for a long time the $H\gamma\gamma$ vertex serves as a "counter" of the particles with masses larger than the Higgs boson mass: if these particles acquire masses due to the standard Higgs mechanism, then they do not decouple from the Higgs boson and provide a constant contribution to the $H\gamma\gamma$ vertex. Therefore, the $H\gamma\gamma$ vertex can provide us, in principle, with unique information about the structure of the theory at energy scales unachievable for modern accelerators.

A similar point also shows up in some other aspect: it turns out that the $H\gamma\gamma$ vertex is very sensitive to different anomalous couplings in the massive gauge boson sector of the Standard Model (SM). All these properties make the $H\gamma\gamma$ interaction vertex an extremely interesting object from the theoretical point of view. In order to exploit the possibility to look for deviations from the SM predictions for the $H\gamma\gamma$ vertex, one needs quite accurate predictions for this vertex within the framework of the Minimal Standard Model.

[6] This statement is also supported by lattice investigations [1]

At the tree level the $H\gamma\gamma$ vertex is absent in the Standard Model. At the one-loop level the W-boson and the top quark contribute to the effective $H\gamma\gamma$ form factor. This one-loop result can be found in the text books [6]. Note for the time being that the contributions of the W and t-quark loop to the $H\gamma\gamma$ vertex have different signs and hence tend to compensate each other. For realistic masses of the W-boson and the top quark this compensation occurs for Higgs boson masses ~ 600 GeV.

The QCD radiative corrections to the $H\gamma\gamma$ vertex were calculated recently by several groups [3]. These corrections are negligible below $t\bar{t}$ threshold and are large above the threshold. As for the size of the other SM radiative corrections, we do not know much about them at present. Recently the corrections of order $O(G_F {m_t}^2)$ were evaluated in the limit of a small Higgs mass [4]. In this paper we consider the leading $O(G_F {M_H}^2)$ SM radiative corrections in the limit of large Higgs boson masses. We show that this correction has the same order of magnitude but the opposite sign as the QCD correction in the interval $0.5\ TeV < m_H < 1.5\ TeV$ and blows up for larger Higgs boson masses.

The technical tool which results in great simplifications of the calculations is the use of the Goldstone Boson Equivalence Theorem (ET) [5].

The organization of the paper is as follows: in section 1 we discuss the one-loop calculation of the $H\gamma\gamma$ vertex in the framework of the ET; section 2 is devoted to the two-loop calculation: we briefly discuss the renormalization procedure and present results for the imaginary and real parts of the $H\gamma\gamma$ vertex; in section 3 we discuss our final results and make some concluding remarks.

2. Lowest order $H\gamma\gamma$ vertex.

The interaction of the Higgs boson with two photons can be described with the help of the effective Lagrangian:

$$L = \frac{\alpha}{4\pi v} F(s) F_{\mu\nu} F^{\mu\nu} H \qquad (1)$$

In this equation $F(s)$ denotes a form factor which contains all information about the particles propagating in the loop. In the Minimal Standard Model the form factor $F(s)$ obtains contributions from the top quark and W-boson

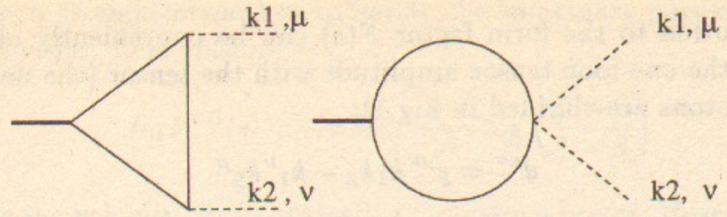

Figure 1: Generic lowest order graphs. The dashed lines correspond to photons, heavy solid lines are Higgs bosons. The particles inside the loop (light solid lines) are W boson and top quark.

The lowest order contribution to the $H\gamma\gamma$ vertex is given by the graphs shown in Fig.1. The analytical results for the fermion and spin-one boson contributions can be found e.g. in [6]. In the limit when the Higgs mass is large in comparison with the mass of the particle propagating in the loop, the contribution of the fermions to $F(s)$ is suppressed as $(\frac{M_f}{M_H})^2$ while the contribution of the W-loop results in a constant :

$$F^{(0)}{}_{m_H \to \infty} \to 2 \qquad (2)$$

This asymptotic value can be obtained using the Goldstone Boson Equivalence Theorem which states that in the limit of a large Higgs mass $M_H \gg M_W$ the leading $O(G_F {M_H}^2)$ contribution to a given Green's function can be obtained by replacing the gauge bosons W, Z by the corresponding would-be Goldsone bosons w, z of the symmetry breaking sector of the theory. The Goldstone bosons can be taken to be massless with the desired accuracy [5].

The interaction of the would-be Goldstone bosons with the Higgs and photon fields is described by the $U_{EM}(1)$ gauged linear σ-model:

$$\begin{aligned} L &= (D_\mu w)^* (D^\mu w) + \frac{1}{2}\partial_\mu z \partial^\mu z + \frac{1}{2}\partial_\mu H \partial^\mu H - \frac{1}{2}{M_H}^2 H^2 \\ &- \frac{{M_H}^2}{4v^2}(\Phi^2 + H^2)^2 - \frac{{M_H}^2}{v}(\Phi^2 + H^2)H - \frac{1}{4}F_{\mu\nu}F^{\mu\nu} \end{aligned} \qquad (3)$$

Here $D_\mu = \partial_\mu - ieA_\mu$ is the $U_{EM}(1)$ covariant derivative, M_H is the mass of the Higgs field, v is its vacuum expectation value and Φ is the triplet of the Goldstone bosons w^+, w^-, z. The Feynman rules for this Lagrangian can be found e.g. in Ref. [7].

Let us first reproduce the result of Eq.(2) using the Lagrangian of Eq.(3). It is straightforward to write down the sum of the Feynman graphs shown in the Fig.1 (neglecting for the moment the contribution from the top loop).

The contribution to the form factor $F(s)$ can be conveniently obtained by contracting the one-loop tensor amplitude with the tensor (the notations for outgoing photons are clarified in Fig.1):

$$d^{\mu\nu} = g^{\mu\nu} k_1 k_2 - k_1{}^{\nu} k_2{}^{\mu} \tag{4}$$

In spite of the fact that the sum of these graphs should be ultraviolet finite, we need to regularize at intermediate steps of the calculation. For simplicity we adopt dimensional regularization, working in d dimensions. At the end of the calculations we shall put d equal to 4. After some algebra one finds for the sum of the lowest order amplitudes:

$$M = M_{\mu\nu} d_{\mu\nu} = M_H{}^2 2\pi\alpha(d-4)s \int \frac{d^d q}{(2\pi)^d} \frac{1}{(k_1+q)^2 (k_2-q)^2} \tag{5}$$

From this equation it is seen that the leading order calculation amounts to the calculation of the divergent part of the massless two-point function. Using well-known results for the two-point function in Eq.(5), we obtain the asymptotic result given in Eq.(2).

It is also possible to calculate these graphs using dispersion relations. In order to do this, we need to cut the graphs shown on the Fig.1 in all possible ways, calculate the contribution of the cut graphs to the imaginary part of the $F(s)$ using unitarity relation and finally integrate the imaginary part of the $F(s)$ along the cut. As our Goldstone bosons are exactly massless, the cut goes from 0 to ∞ in the complex s-plane. If we cut the graphs of Fig.1, the imaginary part of $F(s)$ is given by the convolution of the decay amplitude $H(s) \to w^+ w^-$ with the amplitude $w^+ w^- \to \gamma\gamma$. Note that conservation of the total angular momentum requires equal helicities of both photons in the final state.

It is not difficult to see by exact calculation that the amplitude $w^+ w^- \to \gamma\gamma$ vanishes for massless w^+ and w^- bosons in the equal photon helicity configuration. Therefore the imaginary part of the $F(s)$ is zero and one fails to reproduce the result of the direct evaluation of the Feynman graphs. To find a way out of this paradox we need to investigate the amplitude $w^+ w^- \to \gamma\gamma$ more carefully. For this aim we introduce a mass for the Goldstone bosons which now serves as an infra-red cut-off. The amplitude is then:

$$d^{\mu\nu} M_{\mu\nu}(w^+ w^- \to \gamma\gamma) = ie^2 \frac{2m^2 s^2}{(t-m^2)(u-m^2)} \tag{6}$$

where m is the mass of the Goldstone bosons and t and u are the Mandelstam variables of the process.

It is then straightforward to calculate the imaginary part of the $F(s)$ to the lowest order. One obtains

$$Im F^{(0)}(s) = -\pi M_H{}^2 \frac{4m^2}{s^2} \log\left(\frac{1+\beta}{1-\beta}\right) \tag{7}$$

where β is the velocity of the (massive) Goldstone boson. If we put the mass of the Goldstone boson equal to zero in Eq.(7), the imaginary part of $F(s)$ is zero in accordance with the previous statement. However, the lower limit in the dispersion integral is $4m^2$. In fact, if we consider the imaginary part given by Eq.(7) in the dispersion integral, we can see that in the limit $m \to 0$ the imaginary part of $F(s)$ turns into a δ(s)-function.

Hence, the correct procedure consists in evaluating the dispersion integral with finite Goldstone boson masses and taking the limit $m \to 0$ only after the integration over the cut has been performed.

In this way, we obtain the same result as in Eq.(2) for the real part of $F(s)$, as has been obtained from the known complete expression for $F(s)$ in the large Higgs mass limit or from the direct evaluation of the Feynman graphs with massless Goldstone bosons.

The reason why we have discussed the one-loop calculation of the $H\gamma\gamma$ vertex in some detail is two-fold: first, it serves as a reference point - to justify the use of the Equivalence Theorem for the two-loop calculation; second, in our opinion this calculation shows some unexpected properties (for instance, the evaluation of this one-loop result through the dispersion relations is very similar to the evaluation of the axial anomaly through the imaginary part of the triangle graph [8]. However, we have failed to find deep reasons underlying this similarity).

3.Two -loop contribution to the $H\gamma\gamma$ vertex

3.1 Renormalization

In this subsection we briefly discuss the renormalization procedure which is needed for the evaluation of the two-loop graphs. First note, that as the $H\gamma\gamma$ interaction is absent in the SM lagrangian, the two-loop graphs must be finite after we renormalize all subdivergencies. In other words, to make our two-loop amplitude finite, we need only one-loop counter terms. The latter are constructed according to the following procedure.

The "matter" part of the Lagrangian (Eq.3) contains two independent parameters: the mass of the Higgs field M_H and the vacuum expectation value v. We fix the one-loop counter-terms by requiring the mass of the Higgs field and the vacuum expectation value to be exact one-loop quantities. This requirement eliminates all tadpole graphs and provides us with the counter-terms for all other divergent subgraphs. For instance, self-energies of the Goldstone bosons must be effectively subtracted on mass-shell. Further we will need the counter-terms for the vertecies Hw^+w^- and Hzz which can also be obtained from above requirements.

The next point is the renormalization of the γw^+w^- vertex. As this vertex is convergent, its renormalization is fixed by the renormalization of the Goldstone boson wave function which in turn is fixed by the renormalization of the self-energy operator for the Goldstone boson. This procedure is compatible with the electromagnetic Ward identities of the gauged σ-model.

3.2 Two-particle cuts.

In this subsection we compute the contributions of the two-particle cuts of the graphs presented in Figs. 2-5. The simplest (quasi one-loop) contributions are given by the set of Feynman graphs shown in the Fig.2 and the two-particle cuts of the graphs in Fig.5.

The graphs shown in the Fig.2 are quasi one-loop graphs. As the Hw^+w^- vertex diverges at the one-loop level one needs to bring in counter-terms which can be obtained according to the recipe given above. It is also convenient to consider simultaneously the graphs shown in Fig.2 and the two-particle cuts of the two-Higgs-two Goldstone boson vertex graphs presented in Fig.5. Summing up the contributions of Fig.2, the two-particle cut contributions of the graphs shown in Fig.5 and the one-loop counter-term for the Hw^+w^- vertex, one has:

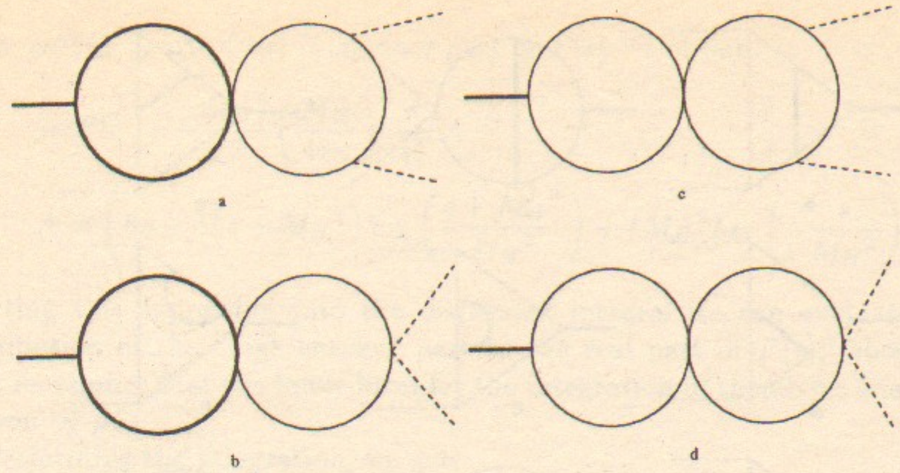

Figure 2: "Quasi one-loop" two-loop diagrams. Heavy solid line denote Higgs bosons, thin solid lines denote w^+,w^-,z goldstone bosons of the ET. Dashed lines are photons.

$$F^{(1)} = 2\left(\frac{M_H}{4\pi v}\right)^2 (2-\sqrt{3}\pi) \tag{8}$$

Next we discuss the contribution of the graphs shown in Fig.3. Note that we are considering only two-particle cuts in this section.

Let us start with the graphs shown in Fig.3(a-b) and consider the two-particle cuts which lie to the right of the virtual Higgs boson line. The cut contribution is given by the convolution of the one-loop $H \to w^+w^-$ amplitude (with the Higgs boson in the t-channel) with the Born amplitude for $w^+w^- \to \gamma\gamma$. As we know from the discussion of the lowest order vertex, the latter is singular for small values of s. Unfortunately, the one-loop correction to $H \to w^+w^-$ is also singular for $s = 0$ if the Goldstone bosons are exactly massless. As before we have to introduce a mass m for the Goldstone boson to handle this infrared divergence. Note at this point, that the ET theorem, guarantees the existence of a smooth limit as $m \to 0$. Hence, we expect that the sum of all two-loop contributions will not be sensitive to the details of the infrared limit of the theory.

Evaluating the Hw^+w^- vertex in the limit $m_H >> \sqrt{s}, m$ we find the following result:

$$F_L = \frac{{M_H}^2}{2}\left(\frac{M_H}{4\pi v}\right)^2 \left(1 + \log\left(\frac{{M_H}^2}{m^2}\right) - \beta \log\left(\frac{1+\beta}{1-\beta}\right)\right) \tag{9}$$

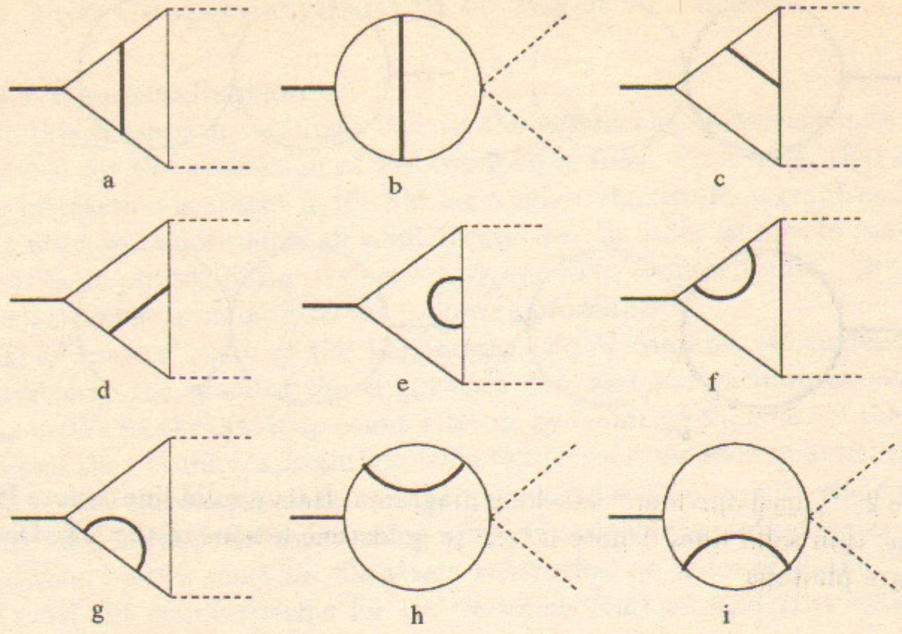

Figure 3: Abelian (QED-like) two-loop diagrams, Line drawings as in Fig.2.

Putting everything together the imaginary part corresponding to the "right cut" graphs of Fig.3(a,b) is given by:

$$ImF^{(2)} = -\frac{{M_H}^2}{2} \cdot 2\pi \frac{4m^2}{s^2} \log\left(\frac{1+\beta}{1-\beta}\right) F_L(s) \qquad (10)$$

Inserting Eq.(10) into a dispersion integral we can evaluate the contribution of these cut graphs to the real part of the $F(s)$ and get:

$$F^{(2)} = 2\left(\frac{M_H}{4\pi v}\right)^2 \left(1 + \log\left(\frac{{M_H}^2}{m^2}\right) - \frac{4}{3}\left(1 + \frac{\pi^2}{12}\right)\right) \qquad (11)$$

Another possibility to cut the graphs Fig.3(a,b) is to cut to the left of the virtual Higgs line. We divide the integration region in the dispersion integral into two parts introducing an arbitrary scale μ. The scale μ can be chosen to satisfy the following inequalities:

$$m \ll \mu \ll M_H.$$

If we are interested in the contribution from the "high – energy" part of this graph, we can put the masses of the Goldstone bosons equal to zero. For the

"high–energy" part of the imaginary part of $F(s)$ we obtain:

$$ImF^{(3)} = -\frac{{M_H}^4}{2}\left(\frac{M_H}{4\pi v}\right)^2 \frac{\pi}{s^3} A$$

$$A = \left(8s - 4\left(s + {M_H}^2\right)\log\left(\frac{s+{M_H}^2}{{M_H}^2}\right) + 4{M_H}^2 Li_2\left(-\frac{s}{{M_H}^2}\right)\right) \qquad (12)$$

Inserting this expression into the dispersion integral we can evaluate the contribution of the "high-energy" part to the real part of $F(s)$, where we must remember that the lower limit for the integration of the above quantity is given by μ.

Performing the integration, we get:

$$F^{(3)} = 2\left(\frac{M_H}{4\pi v}\right)^2 \left(\frac{1}{4}\log\left(\frac{\mu^2}{{M_H}^2}\right) - \frac{7}{2} + \frac{\pi^2}{6} + \frac{3}{2}\zeta(3)\right) \qquad (13)$$

Next we have to find the contribution of the "low-energy" region of this graph to the $F(s)$. We do this by expanding the amplitude in terms of powers of $\frac{\sqrt{s}}{M_H}$ and $\frac{m}{M_H}$.

The result for the imaginary part reads:

$$ImF^{(3)} = -\pi {M_H}^2 \left(\frac{M_H}{4\pi v}\right)^2 \frac{\beta}{s^2}\left(-\frac{s}{2} + 4m^2\left(\frac{\pi^2}{2} - \log^2\frac{1+\beta}{1-\beta}\right)\right) \qquad (14)$$

Inserting (14) into the dispersion integral and integrating from $4m^2$ up to μ^2 we find the "low-energy" contribution to the real part of $F(s)$:

$$F^{(3)} = 2\left(\frac{M_H}{4\pi v}\right)^2 \left(-\frac{1}{4}\log\frac{\mu^2}{m^2} - \frac{5}{6} + \frac{\pi^2}{18}\right) \qquad (15)$$

Finally we have to sum the "low-energy" and "high-energy" contributions and get:

$$F^{(3)} = 2\left(\frac{M_H}{4\pi v}\right)^2 \left(-\frac{1}{4}\log\frac{{M_H}^2}{m^2} - \frac{13}{3} + \frac{\pi^2}{9} + \frac{3}{2}\zeta(3)\right) \qquad (16)$$

The next two-particle cut contributions that we have to consider are obtained by cutting the graphs presented in Fig.3(c,d,e). The calculation proceeds in complete analogy with the case considered in details above. The result of our evaluation is:

$$F^{(4)} = 2\left(\frac{M_H}{4\pi v}\right)^2 \left(-\frac{3}{4}\log\frac{{M_H}^2}{m^2} - \frac{\pi^2}{2} + \frac{3}{2}\zeta(3) + 3\right) \qquad (17)$$

We mention that the graphs Fig.3(f,h,g,i) have no two-particle cuts due to on-shell renormalization of the Goldstone bosons.

If we sum $F^{(2)}$, $F^{(3)}$ and $F^{(4)}$ we see that the sum is finite in the limit $m \to 0$ in agreement with our expectations:

$$F^{(2)} + F^{(3)} + F^{(4)} = 2\left(\frac{M_H}{4\pi v}\right)^2 \left(3\zeta(3) - \frac{\pi^2}{2} - \frac{5}{3}\right) \tag{18}$$

To recapitulate, Eq.(18) contains the contribution of the two-particle cuts of the diagrams in Fig.3.

Next we are going to discuss the two-particle cut contribution corresponding to graphs presented in Fig.4(a-b). Similar to the situation discussed above there are two possible ways of cutting these graphs, i.e. to the left and to the right of the virtual Goldstone boson line.

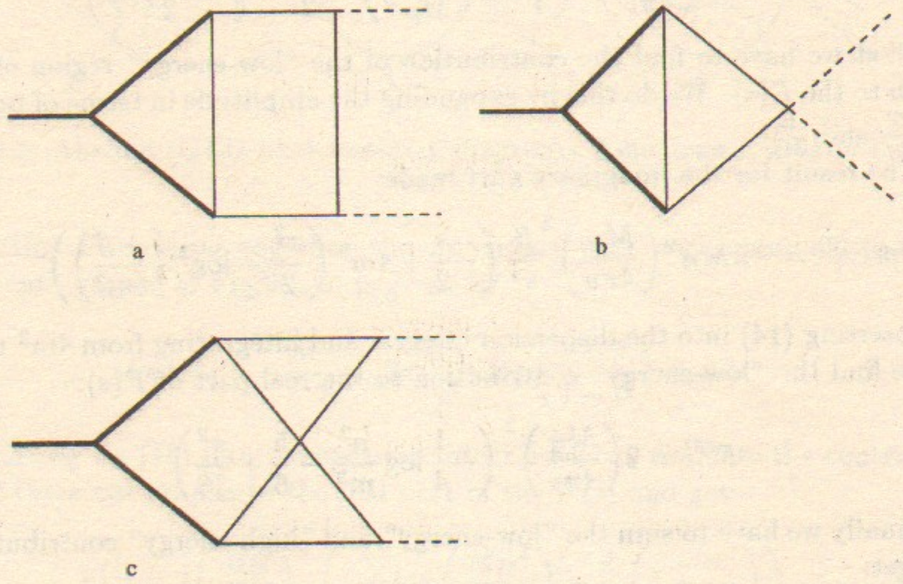

Figure 4: Two loop diagrams with triple Higgs coupling. Line drawings explained in Fig.2

We start with the contribution of the right-cut graph. Its contribution is given by the convolution of the correction to the Hw^+w^- vertex and the $w^+w^- \to \gamma\gamma$ amplitude. In this case the Hw^+w^- vertex is not singular for $s = 0$ when the Goldstone bosons are massless. Hence the contribution of this "right-cut" graph is simply given by the product of the lowest order

$w^+w^- \to \gamma\gamma$ and the Hw^+w^- vertex calculated for $s = 0$. One obtains:

$$F^{(5)} = 2\left(\frac{M_H}{4\pi v}\right)^2 \cdot 3 \tag{19}$$

The contribution of the "left-cut" graphs is also calculated straightforwardly [7]. After a little algebra we find the following result for the imaginary part :

$$Im\, F^{(6)} = \frac{3\pi}{2}\left(\frac{M_H}{4\pi v}\right)^2 \frac{{M_H}^4}{s^2} 2\beta_H \left(\frac{1+{\beta_H}^2}{\beta_H}\log\left(\frac{1+\beta_H}{1-\beta_H}\right) - 2\right) \tag{20}$$

In this equation

$$\beta_H = \sqrt{1 - \frac{4{M_H}^2}{s}}$$

is the velocity of the Higgs boson in the intermediate state. Note, that the dispersion integral starts at the point $s = 4{M_H}^2$. The result of the integration is given by:

$$F^{(6)} = 2\left(\frac{M_H}{4\pi v}\right)^2 \left(\sqrt{3}\pi - \frac{\pi^2}{6} - \frac{15}{4}\right) \tag{21}$$

The next step is the evaluation of the contribution of the graph presented in Fig.4(c). There is only one possibility to obtain a two-particle cut from this graph – it is the cut with the two Higgs bosons in the intermediate state. The evaluation of this cut is much more involved due to its non–planar topology. Some details of our evaluation of this graph are given below.

First, after cutting the graph, we face the necessity to evaluate the box graph. Contracting the box amplitude with the $d_{\mu\nu}$ tensor (defined in Eq.(4)), we find the following representation for the box graph contribution:

$$T_{\mu\nu}d_{\mu\nu} = \frac{i}{(4\pi)^2}\int dydz\left(\frac{2s}{g(y,z)} + \frac{-sm^2 + ({M_H}^2 - t)({M_H}^2 - u)}{g^2(y,z)}\right) \tag{22}$$

[7] There is one subtlety in this discussion. Considering this cut graph more carefully we find both real and **imaginary** parts originating e.g. from the imaginary part of the box graph $HH \to \gamma\gamma$. For our purposes we need only the real part of the amplitude, which (after being integrated over the intermediate particle phase space in the unitarity relation) results in Eq.(20). As for the **imaginary** part of the box graph, it will be exactly canceled by the imaginary part of the **three particle cut**. In the latter case, the imaginary part comes from the pole of the virtual Higgs boson propagator, which comes into play when total energy of the process is larger than $2M_H$ (see also the discussion after Eqs.(38) and (39)).

where s,t,u are the usual Mandelstam variables and the function $g(y,z)$ reads:

$$g(y,z) = m^2 + (u-m^2)y + (t-m^2)z + syz$$

The y and z integrations in Eq.(22) extend from 0 to 1. After integration over y and z we get the following result for the box graph amplitude:

$$M = 4\pi\alpha \cdot i \left(\frac{M_H}{4\pi v}\right)^2 2\left(\log^2\left(\frac{tu - {M_H}^4}{(t-{M_H}^2)(u-{M_H}^2)}\right) - 4Li_2(1) + 2Li_2\left(\frac{tu-{M_H}^4}{(t-{M_H}^2)(u-{M_H}^2)}\right) + Li_2\left(-\frac{(t-{M_H}^2)^2}{tu-{M_H}^4}\right) + Li_2\left(-\frac{(u-{M_H}^2)^2}{tu-{M_H}^4}\right) + \frac{1}{2}\log\left(\frac{-tu}{{M_H}^4}\right)\right) \quad (23)$$

In this equation $Li_2(x)$ is a Spence function as defined in reference [9]. To calculate the contribution of the box to the imaginary part of the formfactor we have to integrate Eq.(23) over two particle phase space. In doing so, it is convenient to introduce a new variable $0 < x < 1$ according to:

$$\frac{s}{{M_H}^2} = \frac{(1+x)^2}{x} \quad (24)$$

Then, the contribution of the box to the imaginary part of the formfactor is given by:

$$ImF^{(7)} = -2 \cdot \frac{3}{2}\left(\frac{M_H}{4\pi v}\right)^2 \frac{{M_H}^4}{s^2}\left(\frac{1-x}{1+x}\left(2\log^2(x) - 2\frac{1+x^2}{1-x^2}\log(x) - 2\pi^2 - 2\right) + 8Li_2(-x) + 2\frac{\pi^2}{3} - 2\log^2(x) + 8\log(x)\log(1+x)\right) \quad (25)$$

Finally, in order to obtain its contribution to the real part of $F(s)$ one needs to integrate the imaginary part along the cut. It is clear from the graphs Fig.4(c) that the cut goes from $4{M_H}^2$ to ∞. Performing this calculation we find:

$$F^{(7)} = -2\left(\frac{M_H}{4\pi v}\right)^2 \frac{3}{2}\left(-\frac{4}{9}\zeta(3) + \frac{38}{27\sqrt{3}}\pi^3 - \frac{23}{9}\pi^2 + \frac{2}{\sqrt{3}}\pi - \frac{11}{6} + 8C_1\right) \quad (26)$$

Here the constant C_1 is :

$$C_1 = \int_0^1 dx \frac{\log(x)\log(x^2+x+1)}{1+x} = -0.194692 \quad (27)$$

The result Eq.(26) completes the list of the two-particle cut contributions.

3.3 Three-particle cuts.

This subsection is devoted to the discussion of the three-particle cuts. First, we consider the graphs corresponding to Fig.3(f,g,h,i). We remind the reader that these graphs have no two-particle cuts due to the on-shell renormalization of the Goldstone bosons. In order to evaluate the three-particle intermediate state contribution, we have to consider the convolution of the two processes $H \to w^+w^-H$ and $(Hw^+)w^- \to \gamma\gamma$. As indicated by bracket the latter process can be viewed as the annihilation of the massless particle w^- and the massive particle (Hw^+) into two photons. It is not difficult to calculate the $d^{\mu\nu}$-contracted amplitude for $(Hw^+)w^- \to \gamma\gamma$ which reads:

$$M^{\mu\nu}\left((Hw^+)w^- \to \gamma\gamma\right) d_{\mu\nu} = ie^2\frac{{M_H}^2}{v} \quad (28)$$

It is then clear that the problem of the calculation of the imaginary part for this cut contribution amounts to the problem of averaging the virtual Goldstone boson propagator on the left side of this graph over three-particle phase space. Performing the integration we find:

$$ImF^{(8)} = -\frac{{M_H}^4}{2}\left(\frac{M_H}{4\pi v}\right)^2 \frac{2\pi}{s^3}\left(-2(s-{M_H}^2) + (s+{M_H}^2)\log\left(\frac{s}{{M_H}^2}\right)\right) \quad (29)$$

We finally substitute this expression into the dispersion integral and integrate along the cut going from $s = {M_H}^2$ to $s = \infty$. The result of this integration is:

$$F^{(8)} = 2\left(\frac{M_H}{4\pi v}\right)^2\left(\frac{13}{8} - \frac{\pi^2}{6}\right) \quad (30)$$

Next we discuss the three-particle cuts of the graphs Fig.3(a,b). Cutting these graphs along the three particle intermediate state contributions, it is easy to see that these graphs produce exactly the same result as the graphs discussed previously (Fig.3 f,h,g,i).

A more non-trivial situation arises for the three-particle cut of the graphs shown on Fig.3(c,d). In this case the complexity stems from the fact that

the amplitude to the right of the cut does not have a simple form as in Eq.(28). The way we proceed is the following: as before we first contract this amplitude with the tensor $d_{\mu\nu}$, and then perform the phase space integration over the momentum of the decay products of the virtual Goldstone boson. Then we obtain the following representation for the imaginary part of $F(s)$:

$$Im F^{(9)} = -\frac{8\pi^2 M_H^2}{s^2}\left(\frac{{M_H}^2}{v}\right)^2 \int \frac{d^3p_2}{(2\pi)^3 2E_2}\frac{\Gamma_2(Q)}{Q^2}\left(\frac{s}{Qk_1}-1\right) \qquad (31)$$

where $Q = k_1 + k_2 - p_2$ and $\Gamma_2(Q)$ is given by

$$\Gamma_2(Q) = \frac{1}{8\pi}\frac{Q^2 - {M_H}^2}{Q^2}$$

Integrating Eq.(31) we obtain the following result for the contribution of this graph to the imaginary part of $F(s)$:

$$Im F^{(9)} = -2\pi\left(\frac{M_H}{4\pi v}\right)^2 \frac{{M_H}^4}{4s^3} A \qquad (32)$$

$$A = \left(2s\log^2\left(\frac{s}{{M_H}^2}\right) - (6s + 2{M_H}^2)\log\left(\frac{s}{{M_H}^2}\right) + 8(s - {M_H}^2)\right)$$

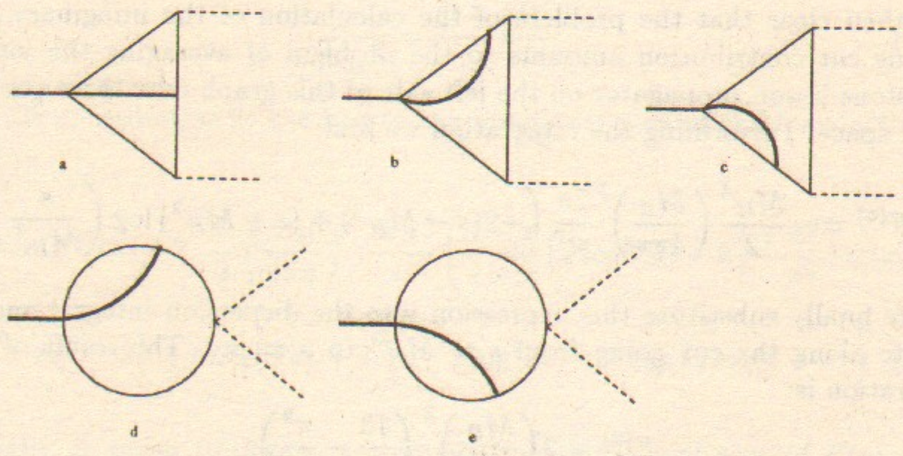

Figure 5: Two-loop diagrams with two Higgs – two Goldstone boson interaction vertices.

Integrating Eq.(32) along the cut we finally obtain the contribution to the real part of $F(s)$ which reads:

$$F^{(9)} = 2\left(\frac{M_H}{4\pi v}\right)^2 \frac{1}{4}\left(\frac{4\pi^2}{3} - \frac{17}{2} - 4\zeta(3)\right) \qquad (33)$$

Next we come to the discussion of the graphs shown in Fig.5. The calculation is performed in complete analogy with the case discussed previously. Without going into details we present the result for the imaginary and real parts of the corresponding cut graphs: The joint contribution of the cut graphs Fig.5(b,d) to the imaginary part is the same as the contribution of the cut graphs Fig.5(c,e) and it has the form:

$$Im F^{(10)} = -2\pi\left(\frac{M_H}{4\pi v}\right)^2 \frac{{M_H}^2}{2s^3}\left(\frac{(s+{M_H}^2)(s-{M_H}^2)}{2} - s{M_H}^2\log\left(\frac{s}{{M_H}^2}\right)\right) \qquad (34)$$

Upon integration we get for the real part:

$$F^{(10)} = 2\left(\frac{M_H}{4\pi v}\right)^2 \left(\frac{\pi^2}{12} - \frac{7}{8}\right) \qquad (35)$$

Next, let us write down the contribution of the cut graph shown in Fig.5a:

$$Im F^{(11)} = -2\pi\left(\frac{M_H}{4\pi v}\right)^2 \frac{{M_H}^2}{4s^3} B \qquad (36)$$

$$B = \Big(-2s{M_H}^2\log^2\left(\frac{s}{{M_H}^2}\right) - 2s{M_H}^2\log\left(\frac{s}{{M_H}^2}\right) + (s-{M_H}^2)(3s-{M_H}^2)\Big)$$

Correspondingly, one has for the real part:

$$F^{(11)} = 2\left(\frac{M_H}{4\pi v}\right)^2 \frac{1}{4}\left(4\zeta(3) + \frac{\pi^2}{3} - \frac{17}{2}\right) \qquad (37)$$

Next we consider the contribution of the three-particle cuts of the graphs shown in Fig.4(a,b). The first step of the calculation is similar to the evaluation of the graphs Fig.5(b-e) because the right-hand side of the cut graph is again given by the simple expression Eq.(28). Performing all further integrations over the phase space variables, we obtain the following representation for the imaginary part of the sum of these cut graphs:

$$Im F^{(12)} = -2\pi\left(\frac{{M_H}^2}{4\pi v}\right)^2 \frac{6{M_H}^4}{s^2}\int_m^{E_{max}} dE \frac{\sqrt{E^2 - {M_H}^2}}{s - 2\sqrt{s}E} \qquad (38)$$

where E_{max} is given by

$$E_{max} = \frac{s + {M_H}^2}{2\sqrt{s}} \qquad (39)$$

One integrates over the energy of the virtual Higgs boson which decays to two Goldstone bosons. The specific feature of this integral is that, depending on the total energy of the process $\sqrt{s}$, the denominator of the integral can go through zero reflecting the fact that an intermediate state with two "real" Higgses can be formed for $s > 4{M_H}^2$. It is also clear that for our purposes we have to treat this singularity in the principal value sense.

It is straightforward to calculate this integral and one obtains the following expression for the imaginary part:

$$ImF^{(12)} = -2\pi\left(\frac{{M_H}^2}{4\pi v}\right)^2 \frac{6{M_H}^4}{s^2}\frac{1}{4}\left(-\frac{1}{2}\log\frac{s}{{M_H}^2} - 1 + \frac{{M_H}^2}{s} + \Psi(s)\right) \tag{40}$$

where the function $\Psi(s)$ is defined by:

$$\Psi(s) = \theta(4{M_H}^2 - s)\frac{3}{2}ctg\left(\frac{\varphi}{2}\right)(\varphi - \frac{\pi}{3}) - \theta(s - 4{M_H}^2)\frac{3}{2}\frac{1-x}{1+x}\log(x) \tag{41}$$

The variable x is defined as in Eq.(24) and φ is defined through the relation

$$s = 4{M_H}^2 sin^2\frac{\varphi}{2}$$

Integrating the imaginary part we finally obtain the following contribution to the real part of $F(s)$:

$$F^{(12)} = 2\left(\frac{M_H}{4\pi v}\right)^2\left(\frac{\pi^2}{8} + \frac{3}{2} - \frac{3\sqrt{3}}{2}Cl_2\left(\frac{\pi}{3}\right)\right) \tag{42}$$

where $Cl_2(\varphi)$ is Clausen's function (see e.g. [9]).

Now we are in the position to discuss the most difficult part of the calculation, namely the evaluation of the contribution of the three-particle cut given by the non-planar graph of Fig.4(c). Performing the integration over the phase space, we obtain the following representation for the contribution of this cut to the imaginary part of $F(s)$:

$$ImF^{(13)} = -2\pi\left(\frac{{M_H}^2}{4\pi v}\right)^2\frac{6{M_H}^4}{s^2}(W_1(s) + W_2(s) + W_3(s)) \tag{43}$$

where W_1, W_2 and W_3 stand for:

$$W_1(s) = 2\left(2\log(2) + \frac{1}{2}\right)\int_m^{E_{max}} dE\frac{\beta_H E}{s - 2\sqrt{s}E} \tag{44}$$

$$W_2(s) = -2\int_m^{E_{max}}\frac{dE}{\sqrt{s}}\frac{s - E\sqrt{s}}{s - 2\sqrt{s}E}\log\left(\frac{s - E\sqrt{s} + \beta_H E\sqrt{s}}{s - E\sqrt{s} - \beta_H E\sqrt{s}}\right) \tag{45}$$

$$W_3(s) = -2\int_m^{E_{max}} dE\frac{\beta_H E}{s - 2\sqrt{s}E}\log\left(\frac{(s - E\sqrt{s})^2}{(\beta_H E\sqrt{s})^2} - 1\right) \tag{46}$$

In this expression E_{max} is defined through Eq.(39) and β_H is the velocity of the Higgs boson:

$$\beta_H = \sqrt{1 - \frac{4M_H^2}{E^2}}$$

In each of the above integrals there is a pole in the integrand for total energies larger than two Higgs bosons masses. We first evaluate each of these integrals in the case when $s > 4{M_H}^2$ and then perform an analytic continuation to the region $s < 4{M_H}^2$. We shall not present explicit expression for the imaginary part of this functions above threshold. If needed, it can be obtained directly from the integral representation of the above functions. One obtains:

$$W_1(s) + W_3(s) = \frac{1}{4}(1 - \frac{{M_H}^2}{s}) - \frac{1}{8}\log\left(\frac{s}{{M_H}^2}\right) + \frac{1}{8}\log^2\left(\frac{s}{{M_H}^2}\right) -$$
$$\frac{{M_H}^2}{2s}\log\left(\frac{s}{{M_H}^2}\right) + \frac{1-x}{2(1+x)}\cdot\left(-\frac{2\pi^2}{3} - 3Li_2(x) - 2Li_2(-x)\right. \tag{47}$$
$$\left. + \frac{7}{4}\log^2(x) - 3\log(x)\log(1-x^2) - \frac{3}{4}\log(x) + \frac{3}{2}\log(x)\log\left(\frac{s}{{M_H}^2}\right)\right)$$

$$W_2(s) = \frac{\pi^2}{6} + \frac{{M_H}^2}{2s}\log\left(\frac{s}{{M_H}^2}\right) - \frac{1}{2}\left(1 - \frac{{M_H}^2}{s}\right)$$
$$+ \frac{1}{8}\log^2\left(\frac{s}{{M_H}^2}\right) - \frac{3}{8}\log^2(x) \tag{48}$$

Here again the variable x is defined by Eq.(24).

Performing the analytic continuation to the region $s < 4{M_H}^2$ we find the following expressions for the above integrals:

$$W_1(s) + W_3(s) = \frac{1}{4}\left(1 - \frac{{M_H}^2}{s}\right) - \frac{1}{8}\log\left(\frac{s}{{M_H}^2}\right) + \frac{1}{8}\log^2\left(\frac{s}{{M_H}^2}\right) -$$
$$\frac{{M_H}^2}{2s}\log\left(\frac{s}{{M_H}^2}\right) + \frac{\cot\left(\frac{\varphi}{2}\right)}{2}\left((\varphi - \frac{\pi}{3})\left(\frac{3}{4} - \frac{3}{2}\log\frac{s}{{M_H}^2}\right.\right.$$
$$\left.\left. + 3\log(2\sin(\varphi))\right) + \frac{1}{2}\left(3Cl_2(2\varphi) - 2Cl_2(\varphi)\right)\right) \tag{49}$$

$$W_2(s) = \frac{{M_H}^2}{2s}\log\left(\frac{s}{{M_H}^2}\right) - \frac{1}{2}\left(1 - \frac{{M_H}^2}{s}\right) + \frac{1}{8}\log^2\left(\frac{s}{{M_H}^2}\right)$$
$$+\frac{3}{8}\left(\varphi - \frac{\pi}{3}\right)^2 \qquad (50)$$

Equations (47-50) provide us with the desired result for the contribution of this graph to the imaginary part of $F(s)$.

The integration in the dispersion integral has to be done numerically and we find:

$$F^{(13)} = -2\left(\frac{M_H}{4\pi v}\right)^2 K, \qquad K = 0.0678 \qquad (51)$$

Summing up all contributions to the real part of $F(s)$ and taking into account permutations of the photon's legs where necessary, we obtain as a final result:

$$\begin{aligned} F &= F^{(0)} + \sum_{i=1}^{6} F^{(i)} + 2\cdot F^{(7)} + 4\cdot F^{(8)} + \\ &+ 4\cdot F^{(9)} + 2\cdot F^{(10)} + 2\cdot F^{(11)} + 2\cdot F^{(12)} + 4\cdot F^{(13)} \\ &= 2\cdot\left(1 - 3.027\left(\frac{M_H}{4\pi v}\right)^2\right) \end{aligned} \qquad (52)$$

The result Eq.(52) completes our calculation and presents the two-loop correction to one-loop result Eq.(2).

4. Discussion and conclusions

Let us finally discuss the phenomenological implications of our results. We begin with a discussion of the one-loop contribution to $F(s)$ in Fig. 6. As mass parameters we have taken $m_t = 180\ GeV$, $m_W = 80\ GeV$. Curve A shows a contribution of the W-boson only, whereas curve B is the sum of the top quark and the W-boson contributions. Fig.6 shows that:

- the contribution of the W-boson to $F(s)$ is slowly approaching its asymptotic value at $m_H > 600\ GeV$
- the contribution of the top quark is important until the Higgs mass reaches the value $m_H \sim 1\ TeV$. We emphasize that there is a strong cancellation between the contributions of the top quark and W boson for Higgs masses of order $m_H \sim 600\ GeV$.

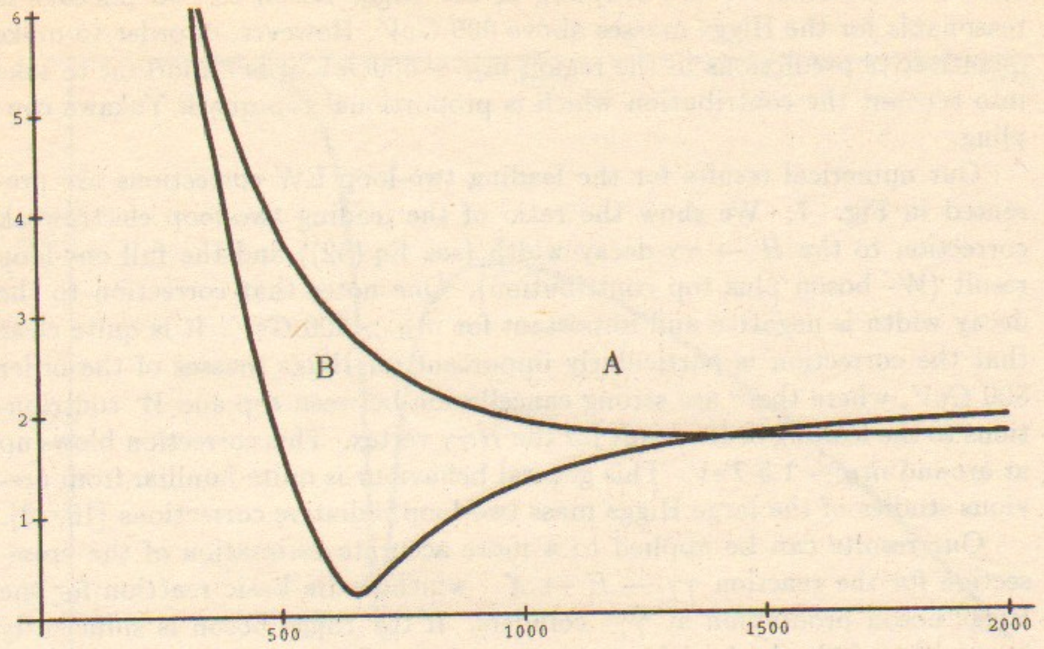

Figure 6: Absolute value of the one-loop form factor of process $H \to \gamma\gamma$, $F(m_H)$, as a function of Higgs mass M_H (GeV). Curve A shows contribution of the W-boson only, whereas curve B is the sum of the top quark and the W-boson contributions.

As a consequence of these observations we expect that, in the two-loop case, the use of the Equivalence Theorem for an estimation of the EW radiative corrections for the coupling of the Higgs boson to two photons is reasonable for the Higgs masses above 600 GeV. However, in order to make quantitative predictions in the region $m_H \sim 600 GeV$ it is important to take into account the contribution which is proportional top quark Yukawa coupling.

Our numerical results for the leading two-loop EW corrections are presented in Fig. 7. We show the ratio of the leading two-loop electroweak correction to the $H \to \gamma\gamma$ decay width (see Eq.(52)) and the full one-loop result (W- boson plus top contribution). One notes that correction to the decay width is negative and important for $m_H > 500\ GeV$. It is quite clear that the correction is particularly important for Higgs masses of the order 600 GeV, where there are strong cancellation between top and W contributions to the leading order result for the $H\gamma\gamma$ vertex. This correction blows up at around $m_H \sim 1.5\ TeV$. This general behaviour is quite familiar from previous studies of the large Higgs mass two-loop radiative corrections [10, 11].

Our results can be applied to a more accurate estimation of the cross-section for the reaction $\gamma\gamma \to H \to X$, which is the basic reaction for the Higgs boson production at $\gamma\gamma$– colliders. If the Higgs boson is sufficiently heavy, than it is the broad resonance with a width growing proportionally to M_H^3. In this case our results for the radiative correction to the on-shell value of the $H\gamma\gamma$ interaction vertex are not sufficient for the description of the Higgs shape in this reaction. However, we have given also results for the imaginary part of the $H\gamma\gamma$ vertex, hence it is straightforward to obtain off-shell value for the $H\gamma\gamma$-vertex, where the dispersion integrates have to be evaluated numerically.

Acknowledgments:

We like to thank J. Gasser for an informative discussion.

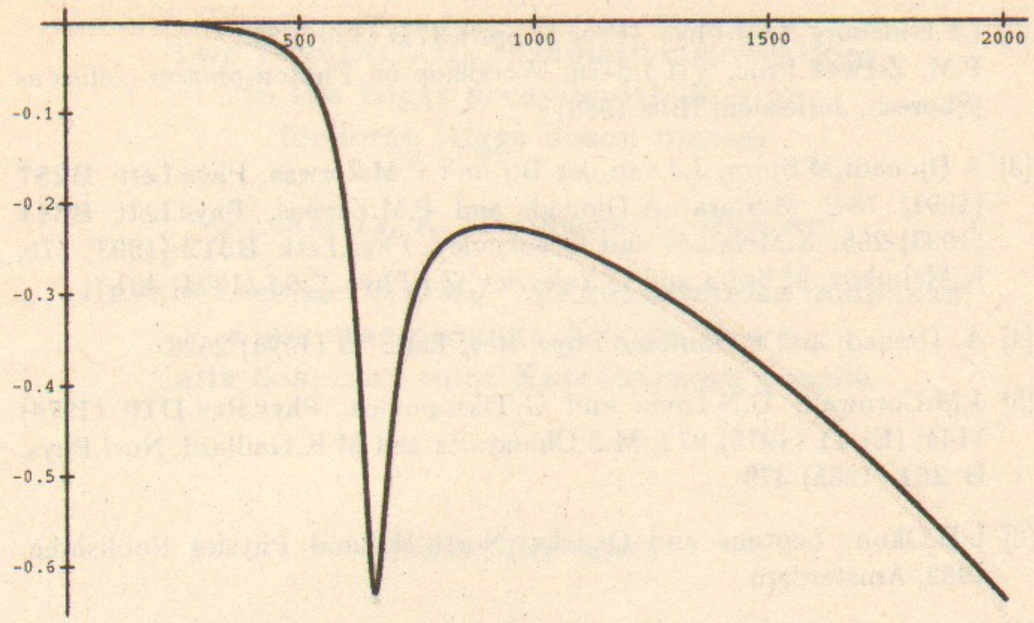

Figure 7: Relative two-loop electroweak correction to the decay width $H \to \gamma\gamma$ (in percent) as a function of M_H (GeV).

References

[1] U.M. Heller et al., Nucl. Phys. B405 (1993) 555

[2] I.F.Ginzburg Nucl.Phys. (Proc.Suppl.) **37B** (1994) 303
P.M. Zerwas Proc. VII Intern. Workshop on Photon-photon collisions (Shoresh, Jerusalem Hills 1988)

[3] A.Djouadi,M.Spira, J.J.van der Bij and P.M.Zerwas, Phys.Lett. **B257** (1991) 187; M.Spira, A.Djouadi and P.M.Zerwas, Phys.Lett **B311** (1993) 255; K.Melnikov and O.Yakovlev, Phys.Lett. **B312** (1993) 179; K.Melnikov, M.Spira and O.Yakovlev, Z.f.Phys. **C64** (1994) 401

[4] A. Djouadi and P.Gambino Phys. Rev. Lett. **73** (1994) 2528

[5] J.M.Cornwall, D.N.Levin and G.Tiktopoulos, Phys.Rev.**D10** (1974) 1145; (E) **11** (1975) 972; M.S.Chanowitz and M.K.Gaillard, Nucl.Phys. **B 261** (1985) 379

[6] L.B.Okun, Leptons and Quarks. North-Holland Physics Publishing, 1982, Amsterdam.

[7] See for instance S.Dawson, "Introduction to the physics of the Higgs boson ". Lectures given at the 1994 Theoretical Advanced Study Institute, Boudler, Co, 1994. Brookhaven preprint BNL-61012, November 1994.

[8] A.D.Dolgov, V.I.Zakharov, Nucl.Phys. **B27** (1971) 525.

[9] L.Lewin. "Polylogarithms and associated functions". Elsevier North Holland, 1981.

[10] J.Fleischer, O.V.Tarasov and F.Jegerlehner, Phys. Lett. B319 (1993) 249

[11] L.Durand, B.Kniehl, K.Riesselmann Phys. Rev. D51 (1995) 5007

J.G. Körner, K. Melnikov, O.I. Yakovlev

Two loop $O(G_F M_H{}^2)$ radiative corrections to the Higgs decay width $H \to \gamma\gamma$ for large Higgs boson masses

Ю. Кёрнер, К. Мельников, О. Яковлев

Двухпетлевые $O(G_F M_H{}^2)$ радиационные поправки к ширине распада Хиггса $H \to \gamma\gamma$ для больших масс Хиггсовского бозона

Budker INP 95-68

Ответственный за выпуск С.Г. Попов
Работа поступила 23.08 1995 г.

Сдано в набор 9.10. 1995 г.
Подписано в печать 9.10 1995 г.
Формат бумаги 60×90 1/16 Объем 1,5 печ.л., 1,2 уч.-изд.л.
Тираж 190 экз. Бесплатно. Заказ N 68

Обработано на IBM PC и отпечатано на
ротапринте ГНЦ РФ "ИЯФ им. Г.И. Будкера СО РАН",
Новосибирск, 630090, пр. академика Лаврентьева, 11.